




## Reassessment of the largest Pleistocene rhinocerotine *Rhinoceros platyrhinus* (Mammalia, Rhinocerotidae) from the Upper Siwaliks (Siwalik Hills, India)

Luca Pandolfi & Leonardo Maiorino

To cite this article: Luca Pandolfi & Leonardo Maiorino (2016): Reassessment of the largest Pleistocene rhinocerotine *Rhinoceros platyrhinus* (Mammalia, Rhinocerotidae) from the Upper Siwaliks (Siwalik Hills, India), *Journal of Vertebrate Paleontology*, DOI: [10.1080/02724634.2015.1071266](https://doi.org/10.1080/02724634.2015.1071266)

To link to this article: <http://dx.doi.org/10.1080/02724634.2015.1071266>

 View supplementary material 

 Published online: 06 Feb 2016.

 Submit your article to this journal 

 Article views: 3

 View related articles 

 View Crossmark data 

## REASSESSMENT OF THE LARGEST PLEISTOCENE RHINOCEROTINE *RHINOCEROS PLATYRHINUS* (MAMMALIA, RHINOCEROTIDAE) FROM THE UPPER SIWALIKS (SIWALIK HILLS, INDIA)

LUCA PANDOLFI\* and LEONARDO MAIORINO

Department of Science, Section of Geology, University of Roma Tre, Largo S.L. Murialdo 1, 00146, Rome, Italy,  
luca.pandolfi@uniroma3.it; leonardo.maiorino@uniroma3.it

**ABSTRACT**—We describe and figure a well-preserved, large skull of a rhinoceros, NHMUK 36661, collected in 1860 from Upper Siwalik deposits. This specimen can be referred to *Rhinoceros platyrhinus*. Comparison with the type material of *R. platyrhinus* revealed that several specimens previously referred to this taxon, including the lectotype, should instead be assigned to *Rhinoceros* sp. (potentially *R. sivalensis* or *R. unicornis*). Therefore, we here provide new detailed cranial and dental characters for *R. platyrhinus*, which is currently known only by a few specimens collected from a restricted area of northern India. We suggest that the generic name *Punjabitherium* erected for *R. platyrhinus* represents a junior synonym of *Rhinoceros* due to the morphological affinities of NHMUK 36661 with *R. unicornis*. A principal component analysis and a cluster analysis confirmed the morphological similarities between *R. platyrhinus* and *R. unicornis*. *Rhinoceros platyrhinus* represents the largest rhinocerotine species in Eurasia and is characterized by a long skull and high-crowned teeth, suggesting that it was a grazer rather than a mixed feeder such as *R. unicornis*. This is supported by a cluster analysis on the upper teeth. The progressive increase in aridity from ca. 12 Ma to Recent in northern India could have affected the dietary regime of *R. platyrhinus* towards to a more grazer-like diet.

**SUPPLEMENTAL DATA**—Supplemental materials are available for this article for free at [www.tandfonline.com/UJVP](http://www.tandfonline.com/UJVP)

Citation for this article: Pandolfi, L., and L. Maiorino. 2016. Reassessment of the largest Pleistocene rhinocerotine *Rhinoceros platyrhinus* (Mammalia, Rhinocerotidae) from the Upper Siwaliks (Siwalik Hills, India). *Journal of Vertebrate Paleontology*. DOI: 10.1080/02724634.2015.1071266.

### INTRODUCTION

The Siwalik Hills, located south of the Himalayas in northwestern India, are mainly composed of Neogene fluvial sediments (Barry et al., 2013, and references therein). However, the term Siwalik Hills is also used to indicate all Neogene fluvial sediments located along the southern margin of the Himalayas and adjacent areas of Pakistan, Nepal, and India (Barry et al., 2013, and references therein; Flynn et al., 2013). The well-known fossil faunas from Siwalik deposits comprise an extraordinary archive upon which the study of the evolution of single taxa and animal communities throughout the Neogene can be based (Falconer and Cautley, 1846; Lydekker, 1876, 1881, 1884; Pilgrim, 1910, 1913; Matthew, 1929; Colbert, 1935; Nanda, 2002, 2008; Flynn et al., 2013). Pilgrim (1910, 1913) divided the Siwaliks into three units: Lower, Middle, and Upper Siwaliks, on the basis of the succession of strata and fossils (Nanda, 2002, 2008; Barry et al., 2013; Flynn et al., 2013). Three species of Rhinocerotidae have been reported from the Upper Siwaliks on the basis of cranial and postcranial material (Falconer and Cautley, 1846; Lydekker, 1876, 1881; Matthew, 1929; Colbert, 1935): *Rhinoceros sivalensis*, *R. palaeindicus*, and *R. platyrhinus*.

*Rhinoceros platyrhinus* was included in the genus *Dicerorhinus* by Pilgrim (1910:201). It was referred to *Rhinoceros* (?*Coelodonta*) *platyrhinus* by Matthew (1929:534) and assigned to the genus *Coelodonta* by Colbert (1935). Colbert (1935, 1942) revised the fossil rhinoceroses from the Siwalik Hills, establishing *R. palaeindicus* as synonymous to *R. sivalensis*, in agreement

with Matthew (1929), and including *R. platyrhinus* in the genus *Coelodonta*. Khan (1971) erected the new genus *Punjabitherium* for this latter species on the basis of a fragmentary skull. Since Khan's contribution (1971), *Punjabitherium platyrhinum* has been frequently used in literature (e.g., Antoine, 2012; Khan et al., 2013). Nevertheless, Prothero et al. (1989) mentioned this taxon as pertaining to *Rhinoceros*, whereas Nanda (2002, 2008) continued to refer it to *Coelodonta*.

*Rhinoceros platyrhinus* material is rare and currently known only from a restricted area, in the surroundings of the Yamuna River and nearby Mirzapur, northern India (Fig. 1). Moreover, several cranial and dental traits of this species were left undescribed or have been poorly investigated. The fossil material reported in Falconer and Cautley (1846) and Murchison (1867), and ascribed to *R. platyrhinus*, includes fragmentary and poorly preserved specimens, whereas the specimen published by Khan (1971) is damaged and lacks several cranial portions.

The goal of this work is to provide a detailed and comprehensive update of the cranial and dental features of one of the largest and rarest rhinoceroses ever discovered in Eurasia and to reassess its systematics. Although this species is still poorly known, its taxonomic status appears critical to better understand the evolution of the Asian taxa. The evolutionary history of Indian and southeastern Asian fossil rhinoceroses is currently confused and poorly investigated. It is unclear how many species of the genus *Rhinoceros* are valid. This issue was a matter of debate during the first half of the 20th century (Matthew, 1929; Colbert, 1935, 1942). A revision of this rhinoceros material would provide new data and thus potentially a new interpretation of the diversity and evolution of fossil rhinoceroses from the

\*Corresponding author.

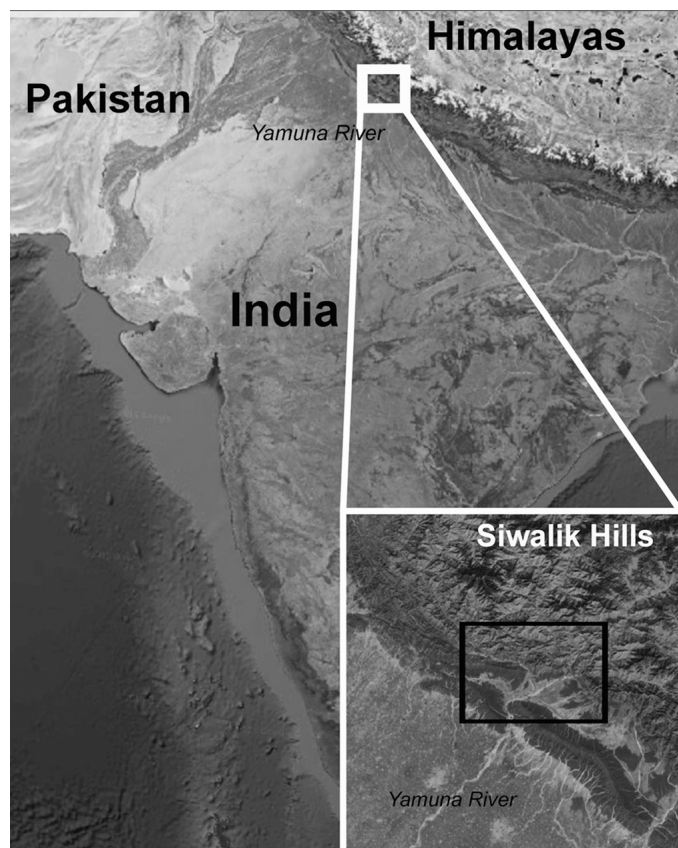


FIGURE 1. Location map of the area where the skull NHMUK 36661 was recovered.

Indian Subcontinent. We also investigated the cranial shape of a large data set of skulls in lateral view ( $n = 169$ ) and upper tooth rows in occlusal view ( $n = 88$ ) of Plio-Pleistocene rhinoceroses of Eurasia by means of geometric morphometrics to further highlight and eventually confirm whether *Rhinoceros platyrhinus* possesses any morphological differences of skull and upper teeth with respect to the other rhinocerotines under investigation.

**Institutional Abbreviations**—AMNH, American Museum of Natural History, New York, U.S.A.; NHMUK Natural History Museum, London, U.K.

## MATERIALS AND METHODS

### Material

This study is based on the description of a well-preserved, large skull currently housed at NHMUK that was collected by Colonel Baker, a collector of many Siwalik fossils (Lydekker, 1881). A short note on this skull was written by Falconer (1868). Later, the specimen was mentioned by Lydekker (1876:29, 1881:49), Colbert (1935:178), and Khan (1971:106). However, as noted by Lydekker (1881:49), this specimen appears to never have been fully described or figured in a scientific work. Lydekker reported a short description of this skull, based on a cast housed in the collection of the Indian Museum, Calcutta (Lydekker, 1881:pls. 8, 9, fig. 2).

In preparation for the geometric morphometric study, we collected photographs of 169 skulls in lateral view and of 88 upper tooth rows in occlusal view of three extant Asian rhinocerotine species (*Dicerorhinus sumatrensis*, *Rhinoceros unicornis*, and *Rhinoceros sondaicus*) and eight extinct rhinocerotine taxa (*Rhinoceros platyrhinus*, *Dihoplus megarhinus*, *Stephanorhinus*

*jeanvireti*, *Stephanorhinus etruscus*, *Stephanorhinus hundsheimensis*, *Stephanorhinus kirchbergensis*, *Stephanorhinus hemitoechus*, and *Coelodonta antiquitatis*) that occur in the Pliocene and Pleistocene fossil record of Eurasia, from both original photos and published pictures. The species list and the number of specimens for each species, as well as the list of institutions where the original specimens are preserved, are reported in Supplementary Data 1. We followed the protocols of Marcus et al. (2000) and Mullin and Taylor (2002) to minimize parallax and measurement error on the photographs.

### Methods

**Morphological Comparison**—The specimen NHMUK 36661 was compared with the rhinocerotid material collected in the same area that has been referred to either *R. unicornis* or *R. sivalensis*, and with the type material of *R. platyrhinus*. Moreover, the studied specimens were compared with several Plio-Pleistocene species of Eurasia as well (Table S1). Comparisons were based on direct observations of material housed at several museums and institutions, as well as specimens published in several contributions (Table S1). Dental and cranial terminology follows Antoine (2002) (Fig. 2), whereas the morphometric methodology follows Guérin (1980).

**Geometric Morphometrics**—Geometric morphometrics is a suitable method for quantifying morphological changes and phenotypic differences among groups of organisms (Adams et al., 2004; Zelditch et al., 2012). Nineteen landmarks and 17 semi-landmarks in two dimensions (Fig. 3A) were digitized on each skull in lateral view, and 18 landmarks on each upper tooth row in occlusal view (Fig. 3B), using tpsDig2 version 2.17 (Rohlf, 2013). Scale bars were used to scale each digitized specimen. Semilandmarks are useful to capture morphological information of outlines where no homologous points can be detected. Curves or contours are assumed to be homologous among specimens (Bookstein et al., 2002; Perez et al., 2006). We digitized semi-landmarks at equal distances along outlines drawn on the specimens. Sexual dimorphism in *Rhinoceros* spp. could potentially influence the shape comparisons among species and affect the results; therefore, we excluded from the landmark configuration the nasal and premaxillary bones, which are known to be sexually dimorphic (Guérin, 1980; Antoine, 2002). Teeth wear down with age, altering the original shape of the crown. Because the specimens represent a range of ages, we collected only upper tooth rows exhibiting little or no wear. We excluded from the data set incomplete or severely damaged skulls or upper tooth rows.

Generalized Procrustes analysis (GPA; Bookstein, 1991) implemented using the procSym() function in 'Morpho' R package (Schlager, 2013) was used to analyze shape among specimens in the cranial and upper tooth row samples. Generalized Procrustes analysis scales, aligns, and rotates each landmark configuration to the unit centroid size (CS = the square root of sum of squared differences between landmarks from their centroid; Bookstein, 1986). Centroid size represents the individual size of specimens. Its variation among rhinocerotines under investigation was visualized using a boxplot.

After GPA, a between-group principal component analysis (bgPCA) was performed on the Procrustes shape variables to identify orthogonal axes of maximal variation in the data set, using the groupPCA() function in 'Morpho' R package (Schlager, 2013). The bgPCA provides a projection of the data onto the principal components of the group means, leading to an ordination of the shape variables between the group means. The new axes are orthogonal and can be computed even when the data are not of full rank, such as for Procrustes shape coordinates (Mitteroecker and Bookstein, 2011). This method offers good performance when the number of cases is smaller than the

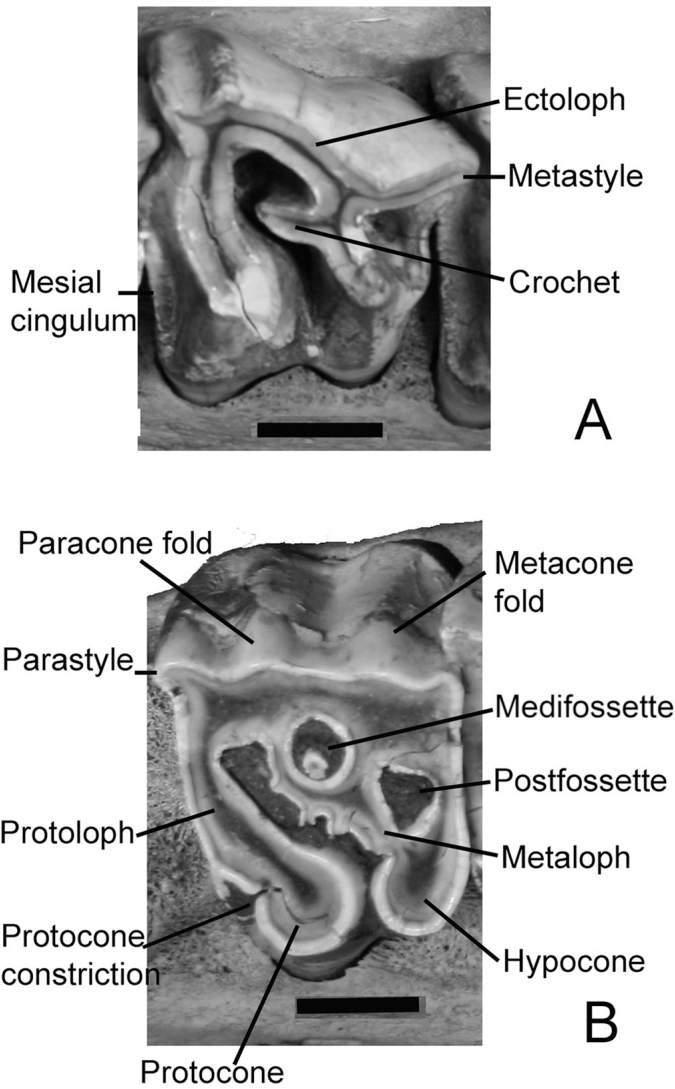


FIGURE 2. Dental nomenclature. **A**, M1 of *Rhinoceros sondaicus* (NHMUK 1861-3-11-1); **B**, P4 of *Rhinoceros unicornis* (NHMUK 19011-3-10-1). Scale bars equal 2 cm.

number of variables, as often occurs in geometric morphometric studies in paleontology (Boulesteix, 2005; Sansalone et al., 2016).

**UPGMA**—A cluster analysis was performed on the shape data of the two data sets to assess similarities among taxa, that is, an UPGMA (unweighted pair group method with arithmetic mean) algorithm performed on the averaged Procrustes distances. The results are two dendrograms of morphological similarities among species included in the sample (skull and upper tooth data sets).

#### SYSTEMATIC PALEONTOLOGY

Order PERISSODACTYLA Owen, 1848  
 Family RHINOCEROTIDAE Gray, 1821  
 Tribe RHINOCEROTINI Gray, 1821  
*RHINOCEROS* Linnaeus, 1758

**Type Species**—*Rhinoceros unicornis* Linnaeus, 1758.

**Other Species**—*Rhinoceros sondaicus* Desmarest, 1822, *Rhinoceros sivalensis* Falconer and Cautley, 1846, *Rhinoceros*

*platyrhinus* Falconer and Cautley, 1846, *Rhinoceros sinensis* Owen, 1870.

**Distribution**—From the Pliocene to Recent of the Indian Subcontinent and southeastern Asia (including southern China).

*RHINOCEROS PLATYRHINUS* Falconer and Cautley, 1846  
 (Figs. 4A–F, S1A, S2A)

**Type Material**—As noted by Lydekker (1876:21, 1881:48), no description of the species was given by Falconer and Cautley (1846). In fact, although most authors refer to Falconer and Cautley (1846) for the taxon name, the description of the type material of *R. platyrhinus* was compiled by Murchison (1867). Additionally, the fossil material was drawn in a plate by Baker and Durand (in Murchison, 1867). Lydekker (1886:100) designated the specimens NHMUK 33662 (fig. 1 of pl. 72 in Murchison, 1867) and M2731 (fig. 2 of pl. 72 in Murchison, 1867) as the types of *R. platyrhinus*. He had previously referred these two specimens to the same skull (Lydekker, 1881:48). In contrast, Matthew (1929:534) indicated the specimens NHMUK 36662 (which is the correct collection number reported on the specimen, reproduced in fig. 1 of pl. 72) as type of the species and NHMUK M2731 (now labeled NHMUK 39628) as the paratype. Matthew (1929) also reported the specimen NHMUK 36661 as the neotype of *R. platyrhinus*. It appears that Matthew (1929) was the first to explicitly designate NHMUK 36661 as the neotype. He essentially ignored the types and derived the morphological characters of the species from NHMUK 36661. Colbert (1935) designated the specimens NHMUK 33662 (= NHMUK 36662), a partial skull (Falconer and Cautley, 1846:pl. 72, fig. 1), as the lectotype of the species and NHMUK M2731 (now labeled as NHMUK 39628) as the cotype and possibly belonging to the same individual as NHMUK 33662. This latter author also considered NHMUK 36661 as the neotype of *R. platyrhinus*. However, although NHMUK 36662 displays morphological characters that suggest an attribution to the genus *Rhinoceros*, it is specifically indeterminate, and NHMUK 36661 should be reconsidered the neotype of *R. platyrhinus* (International Commission on Zoological Nomenclature [ICZN] Recommendation 75A and D).

**Type Locality and Horizon**—Upper Siwaliks, from the Early Pleistocene to early Middle Pleistocene, Siwalik Hills, in the surrounding areas of Yamuna River, northern India.

**Distribution**—The species is known only from the type area and from the vicinity of the town Mirzapur (northern India).

**Referred Material**—An almost complete and well-preserved skull, NHMUK 36661.

**Emended Diagnosis**—The largest species of the genus *Rhinoceros*; the skull is high and massive; presence of lateral apophyses on the nasal bones; nasal notch above P3; infraorbital foramen above P3–P4; anterior border of the orbit above the M1–M2 contact; occipital face straight, cheek teeth high-crowned; P3–M2 with paracone and metacone folds; M1–M2 with medifossette. Differs from *R. unicornis*, *R. sondaicus*, *R. sivalensis*, and *R. sinensis* in having longer skull and cheek teeth. Differs from *R. unicornis* in having a marked metacone fold on M1–M2 and in lacking a medifossette on the premolars. Differs from *R. sondaicus*, *R. sivalensis*, and *R. sinensis* in having high-crowned cheek teeth, a metacone fold, and a medifossette on M1–M2.

#### DESCRIPTION

**Skull**—The skull is massive in lateral view (Fig. 4A). The dorsal profile of the skull is concave, the nasal bones are dorsally convex, the insertion of a nasal horn is evident, and a lateral apophysis is present on the ventral border of the

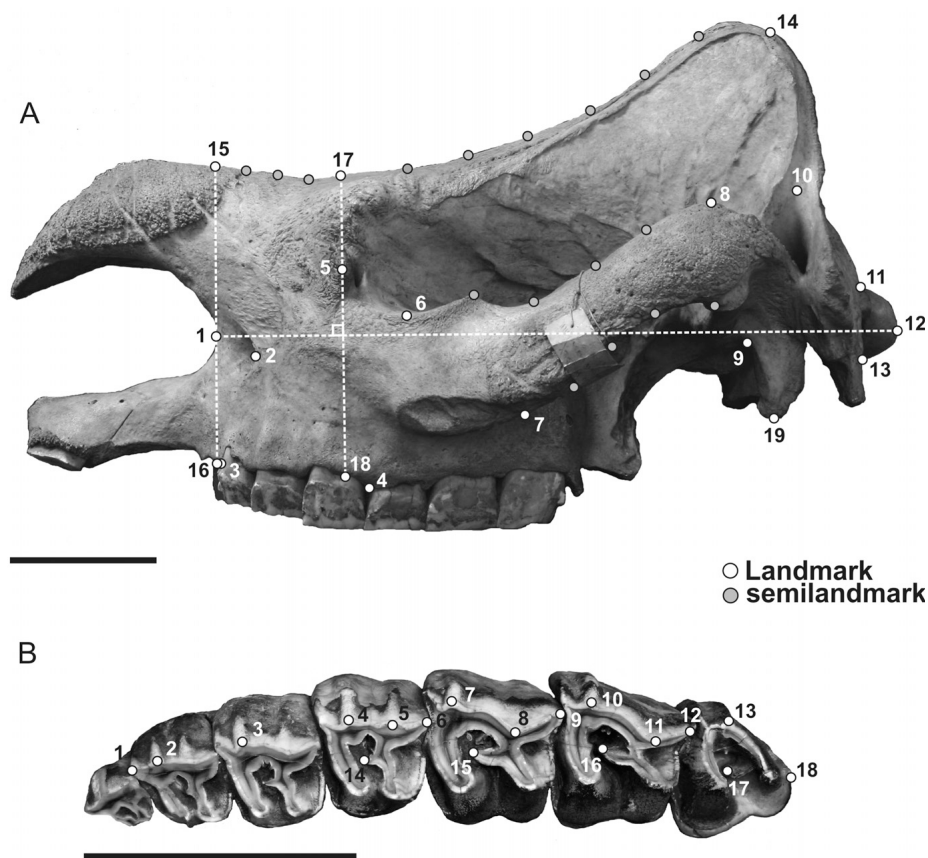


FIGURE 3. Landmark and semilandmark configurations. **A**, landmark configurations for skull in lateral view (*Rhinoceros unicornis*, NHMUK 1972–739): (1) posterior border of nasal notch; (2) infraorbital foramen; (3) anterior border of P2; (4) posterior border of upper premolar row; (5) anterior border of orbit; (6) lower tip of orbit; (7) maximum curvature point of ventral border of zygomatic arch; (8) dorsal tip of zygomatic arch; (9) anterior border of the postglenoid process at its junction; (10) junction between temporal and nuchal crests; (11) dorsal tip of occipital condyle; (12) posterior tip of occipital condyle; (13) ventral tip of occipital condyle; (14) maximum curvature point of posterior area of nuchal crest; (15) projection of landmark 1 on dorsal border of nasal bones; (16) projection of landmark 1 on ventral border of premaxillary/maxillary bones; (17) projection of landmark 5 on dorsal border of frontal bones; (18) projection of landmark 5 on ventral border of maxillary bones; (19) ventral tip of postglenoid process; **B**, landmark configurations for upper tooth row (*Rhinoceros sondaicus*, MNHN PeE 588): (1) anterior-most tip of upper tooth row, excluding P1/DP1; (2) tip of paracone fold of P2; (3) tip of paracone fold of P3; (4) tip of paracone fold of P4; (5) metacone fold or groove of P4; (6) metastyle of P4; (7) apex of paracone fold of M1; (8) metacone fold or groove of M1; (9) metastyle of M1; (10) tip of paracone fold of M2; (11) metacone fold or groove of M2; (12) metastyle of M2; (13) tip of paracone fold of M3; (14) crochet of P4; (15) crochet of M1; (16) crochet of M2; (17) crochet of M3; (18) posterior end of upper tooth row. Scale bars equal 10 cm.

nasals (Fig. 4A). The nasal notch is ‘U’-shaped, and its posterior end lies above P3. The infraorbital foramen is large and located above the P3–P4 contact. The anterior border of the orbit lies above the M1–M2 contact, the zygomatic arch is relatively massive, and the lacrymal process is present (Fig. 4A). The external auditory pseudomeatus is closed, and the occipital face is straight. The horn does not insert on the frontal bones (Fig. 4A). A sagittal crest extends onto the basilar process in basal-occipital view (Fig. 4B). The posterior border of the nuchal crest is concave and the frontal-parietal crests are well separated in dorsal view. In occipital view, the occipital face is trapezoidal, the dorsal border of the nuchal crest displays a concavity in the middle, the foramen magnum is circular, and the occipital condyles are relatively large (Fig. 4C, D). The area between the occipital lateral crests and the lateral-external crests is enlarged and appears inflated (Fig. 4D).

**Teeth**—The cheek teeth are hypsodont, the lingual and labial cingula are absent, and the paracone and metacone folds are evident on premolars, M1, and M2 (Fig. 4E, F). The alveoli of a P1 or a DP1 are evident.

In occlusal view, P2s display a relatively long crista and a small crochet. The protoloph is joined with the ectoloph, and the protocone is constricted (Fig. 4E, F). Moreover, the protocone and the hypocone have a short contact lingually, the metaloph appears ‘S’-shaped, and the postfossette is large and posteriorly closed.

The metaloph is ‘S’-shaped, and the protoloph is oblique on P3s; the protocone and hypocone are lingually joined, whereas the crista is small and the crochet is well-developed with an accessory fold (Fig. 4E, F). The parastyle is relatively long and narrow.

The protocone and hypocone of P4 are joined at a slightly advanced stage of wear (Fig. 4E, F). The mesial cingulum is evident. The crista appears absent on the right P4, but is present on the left. The crochet is small and narrow (Fig. 4E, F). The metaloph is wavy in occlusal view, and the hypocone is constricted.

The medifossette is closed, the protoloph and the metaloph bend backwards distally on M1 (Fig. 4E), the protocone is constricted, and the postfossette is smaller than that on P3–P4 (Fig. 4E, F).

The medifossette is closed on M2, and an accessory fold is present on its anterior border (Fig. 4E, F). Protoloph and metaloph turn backward lingually. An incipient mesostyle is evident.

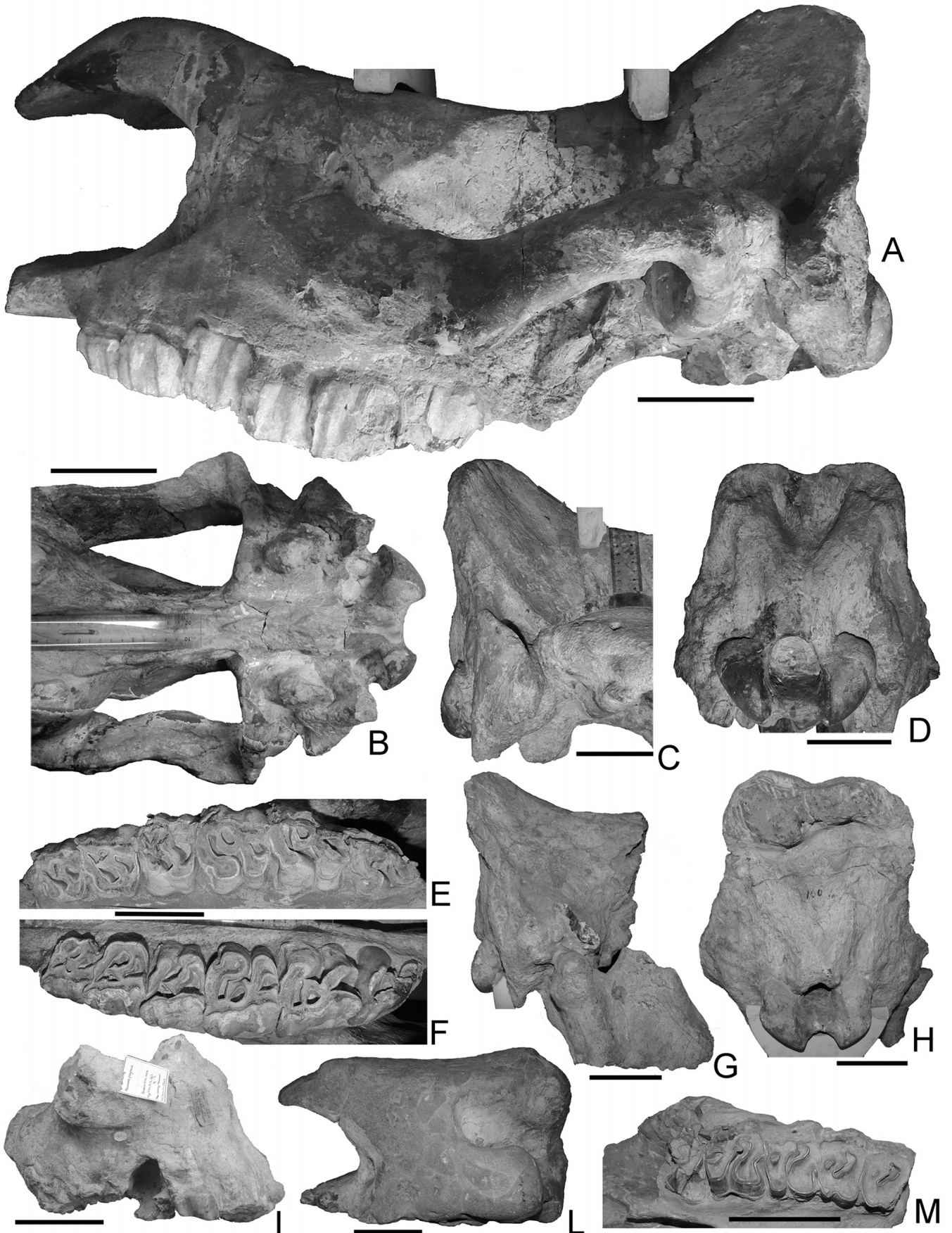
The M3s display a small crista, a single crochet, a slightly constricted protocone, and a marked paracone fold (Fig. 4E, F).

## RESULTS

### Morphological Comparison with *Rhinoceros*

Fossil remains of *Rhinoceros* have been recorded in several localities of the Indian Subcontinent and southeastern Asia (Table S1; Antoine, 2012, and references therein).

**Comparison with *Rhinoceros unicornis***—In comparison with NHMUK 36661, the skull of *R. unicornis* (Tables S1, S2) is shorter in lateral view, with a forward-leaning occipital face. In *R. unicornis*, the posterior border of the nasal notch is above P2 or the contact between P2 and P3, the infraorbital foramen lies above P3, and the anterior border of the orbital cavity is located above the P4–M1 contact or M1 (Fig. S1). The skull of *R. unicornis* and NHMUK 36661 have several features in common: a dorsal concave profile of the skull,



a convex profile of the nasal bones, the presence of the nasal horn insertion, a closed external auditory pseudomeatus, the presence of the lacrymal process, the presence of a slight concavity in the middle of the dorsal and posterior borders of the nuchal crest, and a high occipital face (Fig. S1). The upper cheek teeth of *R. unicornis* differ from those of NHMUK 36661 in having a closed medifossette with an accessory fold on the premolars and a shallow metacone fold on M1 and M2 (Fig. S2).

**Comparison with *Rhinoceros sondaicus***—*R. sondaicus* (Table S1) has a dorsoventrally shorter occipital face in occipital view, a posterior border of the nasal notch lying above P2, and an infraorbital foramen above the P3 (Fig. S1). The anterior margin of the orbit is located above P3–P4 or P4 in *R. sondaicus*, and the occipital face leans forward in lateral view. The upper cheek teeth of *R. sondaicus* are low-crowned and differ from those of NHMUK 36661 in having separated protocone and hypocone and parallel protoloph and metaloph on the premolars (Fig. S2). Moreover, the metacone fold is absent on M1 and M2 and is shallow or absent on the premolars, the crista is usually absent on the teeth, and the medifossette does not occur on the molars (Fig. S2).

**Comparison with *Rhinoceros sivalensis***—Cranial material of *R. sivalensis* is poorly known, being represented by only a few specimens collected from the Siwalik Hills (Table S1; Falconer and Cautley, 1846; Colbert, 1935). This species has been considered a synonym of *R. unicornis* (Antoine, 2012). Compared with the specimen studied here, the type material of *R. sivalensis* shows the anterior border of the orbit lying above P4–M1, the posterior end of the nasal notch lying above P2, and separated protocone and hypocone on P4. Moreover, the medifossette is absent on the molars, and the crista is absent on the premolars (Fig. S2). The specimens originally referred to *R. palaeindicus* in Falconer and Cautley (1846) are rather similar to *R. sivalensis*. They differ from the type specimen of *R. sivalensis* in having a pronounced lingual cingulum on P2–P4, a small crista on M1, a long crista on P3, a postfossette distally opened on P3–P4, and protoloph and metaloph lingually convergent on P3.

**Comparison with *Rhinoceros sinensis***—The taxonomic status of *R. sinensis* is still debated (Antoine, 2012, and references therein). The comparison is here based on material published by Matthew and Granger (1923) and Colbert and Hooijer (1953). The M1 and M2 of *R. sinensis* differ from those of NHMUK 36661 in the lack of the medifossette and metacone fold, and in having a concave posterior profile of the ectoloph. The protocone and hypocone are separated on P3–P4 in *R. sinensis*, whereas the metaloph and protocone are not constricted. In addition, the protoloph and metaloph are lingually convergent on P2, which is triangular in shape (Matthew and Granger, 1923).

**Comparison with *Rhinoceros platyrhinus***—Within the type material of *R. platyrhinus*, the cranial fragment NHMUK 39628 (=NHMUK M2731) is a dorsally deformed occipital area only (Fig. 4G, H). The foramen magnum is circular in occipital view. The occipital face is high, and the dorsal border of the occipital crest possesses a concavity in the middle as in the studied specimen (Fig. 4C, D). It further displays a closed external auditory pseudomeatus and a straight occipital face in lateral view. In dorsal view, the nuchal crest is slightly concave as in NHMUK 36661.

In NHMUK 39643, the skull is fragmentary and poorly preserved (Fig. 4I). The anterior border of the orbit lies above the P4–M1 contact, and the infraorbital foramen lies above the P2–P3 contact. The teeth are heavily worn in NHMUK 39643 and differ from those of NHMUK 36661 in having separated protocone and hypocone on P4, absence of a metacone fold on P4, presence of a strongly constricted protocone on M3, and presence of an antecrochet on M3. Specimen NHMUK 39643 is more similar to *R. sivalensis* instead.

The specimen NHMUK 36662 is eroded and polished and poorly preserved (Fig. 4L, M). In lateral view, the infraorbital foramen is relatively large. The lacrymal process appears to be absent, and the anterior margin of the orbit lies above M1. The upper cheek teeth of NHMUK 36662 (Fig. 4M) differ from those of NHMUK 36661 in the lack of the closed medifossette on M1 and M2 and in having a small crochet on M1 and M2. Moreover, NHMUK 36662 lacks the metacone fold on M2, which displays a concave posterior profile of the ectoloph, and a metaloph bends backwards distally on M1. Unfortunately, the premolars are heavily worn and a further comparison is not possible, but the few recognized characters suggest an attribution to *R. sivalensis*.

An isolated M3 (NHMUK 39669) resembles those of NHMUK 36661 in having a long and curved crochet, a shallow and wide paracone fold, and a reduced distal cingulum on the hypocone.

An isolated M2 (NHMUK 39641) displays a large and well-developed crochet with an accessory fold, an apparent medifossette (the crista appears absent and the medifossette is formed by an accessory fold of the crochet), a constricted protocone, and an apparently very shallow metacone fold. The morphology of this tooth resembles that of *R. unicornis* rather than that of NHMUK 36661.

The fragmentary skull (A/559; Department of Geology, University of Punjab) described and figured by Khan (1971) displays, in lateral view, a concave dorsal profile, a lacrymal process, an anterior border of the orbit located above the M1–M2 contact, a posterior end of the nasal notch presumably lying above P3, and a closed external auditory pseudomeatus. All of these characters are shared with NHMUK 36661. Unfortunately, the occipital face is badly damaged so that several anatomical features cannot be observed. Moreover, we maintain that the slight inclination of the occipital face, evident in lateral view, is an artifact of the taphonomic deformation of the skull. The occipital foramen is circular in occipital view, and a sagittal crest is evident on the basilar process of the basioccipital view. Only the M3s are preserved, but they are rather worn. Remarkable characters are the presence of a small crista and a crochet. These latter features are evident on the M3s of AMNH 19777 (Colbert, 1935:fig. 78). Colbert (1935:fig. 78) referred three specimens to *Coelodonta platyrhinus*: AMNH 19777, 19875, and 19822. The specimens AMNH 19777 and AMNH 19875 share several characters with NHMUK 36661, such as a closed medifossette on M1 and M2 with accessory folds, backward protoloph and metaloph on M2, and a protocone constriction on M1. The length of the molar row of AMNH 19777 (M1–M3 = 175 mm) is slightly shorter than that of NHMUK 36661, but it is longer than those of several Eurasian species (Table S2). The specimen AMNH 19822 is represented by deciduous teeth, and certain attribution to *R. platyrhinus* appears doubtful.

←FIGURE 4. *Rhinoceros platyrhinus* from Upper Siwaliks, Yamuna River, northern India. **A–F**, skull NHMUK 36661. **A**, lateral view; **B**, ventral view of basicranium; **C**, lateral view of occipital area; **D**, occipital view; **E**, occlusal view of left tooth row; **F**, occlusal view of right tooth row; **G, H**, fragment of skull NHMUK 39628 (= NHMUK M2731). **G**, lateral view; **H**, occipital view; **I**, fragment of skull NHMUK 39643 in lateral view; **L, M**, fragment of skull NHMUK 36662. **L**, lateral view; **M**, occlusal view of right tooth row. The specimen NHMUK 36662, belonging to the type material of *R. platyrhinus*, is here referred to *Rhinoceros sivalensis*. All scale bars equal 10 cm.

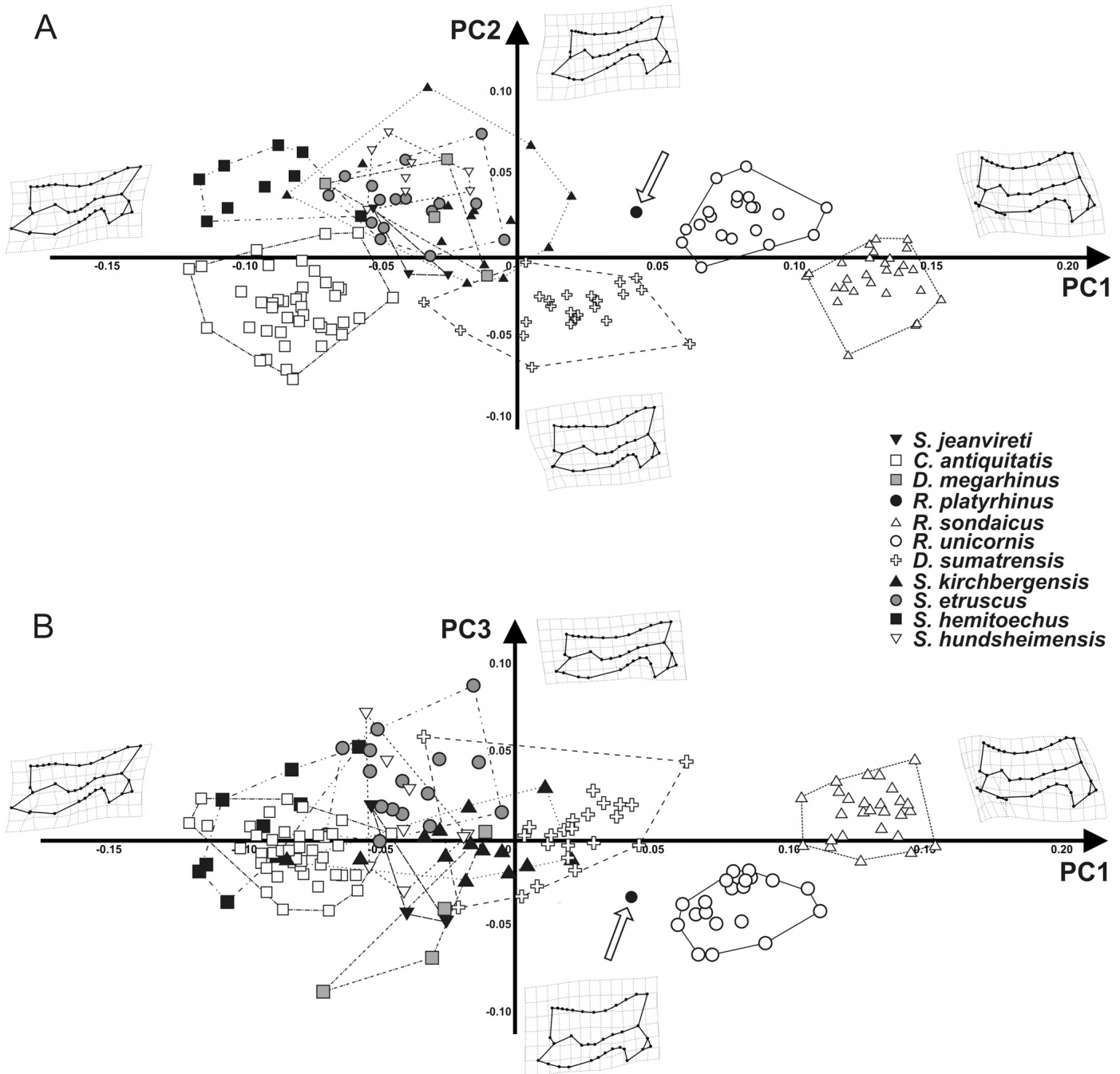


FIGURE 5. A between-group principal component analysis performed on the skulls in lateral view. **A**, relationship between PC1 and PC2; **B**, relationship between PC1 and PC3. The white arrows indicate the position of *Rhinoceros platyrhinus* in the morphospace.

### Geometric Morphometrics

**Cranial Shape Variation**—The first five principal components of the bgPCA performed on the skulls, explain 97% of total shape variance. Figure 5A shows the relationship between PC1 (75.46% of the total shape variance explained) and PC2 (11.33% of the total shape variance). In Figure 5B, we show the plot between PC1 and PC3 (the latter corresponding to 5.13% of the total shape variance). Positive PC1 values are associated with a short skull having a short upper tooth row, starting at the level of the nasal notch, short nuchal crest, a strongly concave dorsal profile, a long zygomatic arch, and an

anterior border of the orbit close to the posterior end of the nasal notch. This cranial morphology is *Rhinoceros*-like. Negative PC1 values are associated with a long skull, having a long upper tooth row, starting rostrally with respect to the nasal notch, a long nuchal crest, a slightly concave dorsal profile, a shorter zygomatic arch, and an anterior border of the orbit less close to the nasal notch. This morphological arrangement is typical of *Coelodonta-Stephanorhinus*.

At positive PC2 values, the skull is long, with a slightly concave dorsal profile, the orbit close to the nasal notch, a long zygomatic arch, a moderately long nuchal crest, and a long upper tooth row, starting anteriorly relative to the nasal notch.



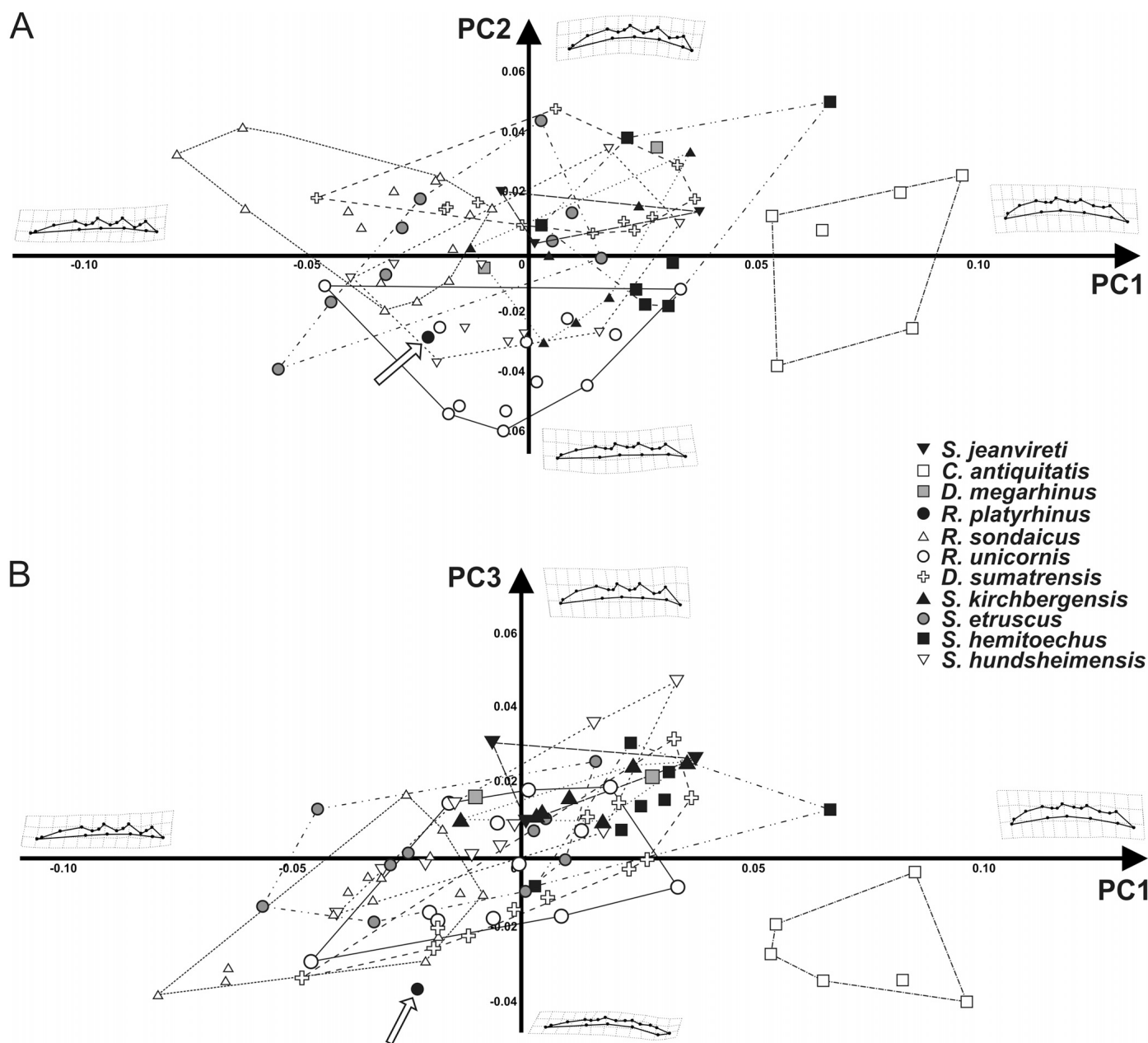


FIGURE 6. A between-group principal component analysis performed on the upper teeth in occlusal view. **A**, relationship between PC1 and PC2; **B**, relationship between PC1 and PC3. The white arrows indicate the position of *Rhinoceros platyrhinus* in the morphospace.

Negative PC2 values reflect a skull that is slightly longer, having a concave dorsal profile, an orbit less close to the nasal notch, a moderately long nuchal crest, a shorter zygomatic arch, and a shorter upper tooth row, starting at the height of the nasal notch.

A low skull with a moderately concave profile, slender zygomatic arch, and a long tooth row is associated with positive PC3 values. The skull is high and has a moderate concave profile, long tooth row, a more massive zygomatic arch, and an anterior border of the orbit close to the nasal notch at negative PC3 values.

In summary, extant *Rhinoceros* spp. and *Dicerorhinus* are mostly associated with positive PC1 values, whereas Eurasian Plio-Pleistocene rhinoceroses occur primarily at negative PC1 values. *Coelodonta antiquitatis* and *S. hemitoechus* lie at extreme negative PC1 values. *Rhinoceros platyrhinus* lies close to *R. unicornis* at positive PC1 values in the morphospace of skulls.

**Tooth Shape Variation**—The first eight principal components of the bgPCA, performed on the upper tooth rows in lateral view, explain 97.9% of total shape variance. Figure 6A shows the relationship between PC1 (50.84% of the total dental shape variance) and PC2 (19.62% of the total dental shape variance), and Figure 6B that between PC1 and PC3 (the latter corresponding to 11.77% of the total dental shape variation). At positive PC1 values, the upper tooth row is grazer-like, slightly labially convex, bearing squared premolars and molars, and has a large M3. At negative PC1 values, the upper tooth row is saw-like, typical of browsers, with a small M3, and a concave posterior profile of the ectoloph. Positive PC2 values are associated with a labially convex upper tooth row having a saw-like profile, small M3, and a paracone fold protruding labially, whereas negative PC2 values are associated with an almost straight upper

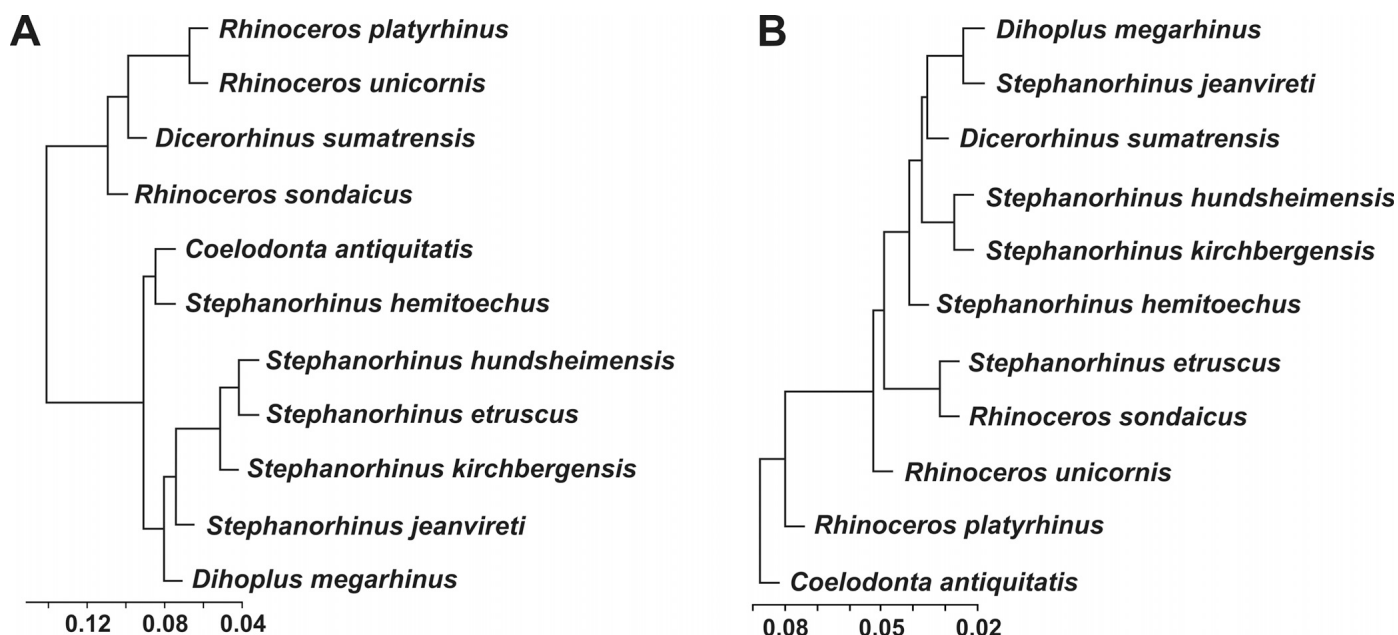


FIGURE 7. UPGMA cluster analysis performed on the two samples. **A**, UPGMA cluster analysis of skulls in lateral view; **B**, UPGMA cluster analysis performed on upper teeth in occlusal view.

tooth row with a less pronounced saw-like profile, a large M3, and a less labially prominent paracone fold.

An upper tooth row with a saw-like profile, a large M3, and a paracone fold protruding labially corresponds to positive PC3 values. An upper tooth row having a less pronounced saw-like profile, a small M3, and concave posterior profile of the ectoloph corresponds to negative PC3 values.

In summary, the Pleistocene Eurasian grazer *C. antiquitatis* varies mainly along positive PC1 values, whereas the extant *R. sondaicus* varies mainly along negative PC1 values, along with *S. etruscus*. The extant *D. sumatrensis* lies at the positive PC2 values of the morphospace, whereas *R. unicornis* lies at the negative PC2 values of the morphospace, along with *S. hundsheimensis*. *Rhinoceros platyrhinus* lies close to *Rhinoceros* spp. in the morphospace at low negative PC1 values and negative PC2 values, but is separated from other rhinocerotine taxa at negative PC3 values.

### Cluster Analysis

In the UPGMA dendrogram of averaged cranial shape similarities (Figure 7A), *R. platyrhinus* clusters with *R. unicornis* and the other two extant Asian rhinoceroses, *R. sondaicus* and *D. sumatrensis*. Plio-Pleistocene rhinoceroses cluster together, indicating similar morphology. The grazer *C. antiquitatis* lies close to the mixed feeder *S. hemitoechus*. All these taxa are well separated from *Rhinoceros* spp. In contrast, when considering the averaged upper tooth row shape values per species (Fig. 7B), *R. platyrhinus* shows a much more grazer-like morphology than extant *R. unicornis*. Browser taxa cluster together, suggesting similar tooth shape.

The boxplot computed for the CS (Fig. 8) shows that *R. platyrhinus* is the largest taxon among Plio-Pleistocene rhinoceroses.

### DISCUSSION

Although Falconer and Cautley (1846) are historically considered as the authors who established several *Rhinoceros* species, including *Rhinoceros platyrhinus*, they never provided a diagnosis for this species and did not indicate a type (see Systematic

Paleontology). Several fragmentary rhinoceros specimens collected from the Siwalik Hills have been reproduced inset into Baker and Durand (in Murchison, 1867). Lydekker (1886) designated NHMUK 33662 and M2731 as the types of *R. platyrhinus*. Matthew (1929) and Colbert (1935) considered a fragment of a skull (NHMUK 36662 = NHMUK 33662) as the lectotype of *R. platyrhinus*. Although these authors considered this specimen to be the anterior portion of the skull of NHMUK M2731 (now labeled as NHMUK 39628), these two specimens are in different states of preservation, and it is unlikely that they pertain to the same individual.

Moreover, within the type material, the specimens NHMUK 36662 and 39643 and the isolated M2 NHMUK 39641 resemble *R. unicornis* or *R. sivalensis*, whereas they are morphologically different from the cranium NHMUK 36661, the skull published by Khan (1971), and the cranial fragment NHMUK 39628. The latter is the only specimen within the type material indicated as *R. platyrhinus* that does not display morphological traits similar to those shown by *R. unicornis* or *R. sivalensis*.

The skull NHMUK 36661 was collected in 1860 and, despite its almost perfect state of preservation, it has never been figured and thoroughly described (Lydekker, 1881). Matthew (1929) and Colbert (1935) erected it as a neotype for *R. platyrhinus*, but provided neither a description nor figures. This choice is in contrast with ICZN rules (Article 75, 75.1) because the authors established a lectotype as well. Nevertheless, the lectotype erected by Matthew (1929) and Colbert (1935) can be referred to a different taxon than *R. platyrhinus* on the basis of morphology. Therefore, following Recommendation 75A and D of the ICZN code, the specimen here described (NHMUK 36661) should be reconsidered as a valid neotype.

Comparison with several specimens referred to different Eurasian Plio-Pleistocene genera clearly indicate that the skull NHMUK 36661 cannot be attributed to *Dicerorhinus*, *Coelodonta*, or *Stephanorhinus* (Supplementary Data 1). This specimen shares many morphological characters with the genus *Rhinoceros* and with some specimens considered as *R. platyrhinus* by Falconer and Cautley (1846) and Colbert (1935). The latter species has been considered as belonging to a different genus,

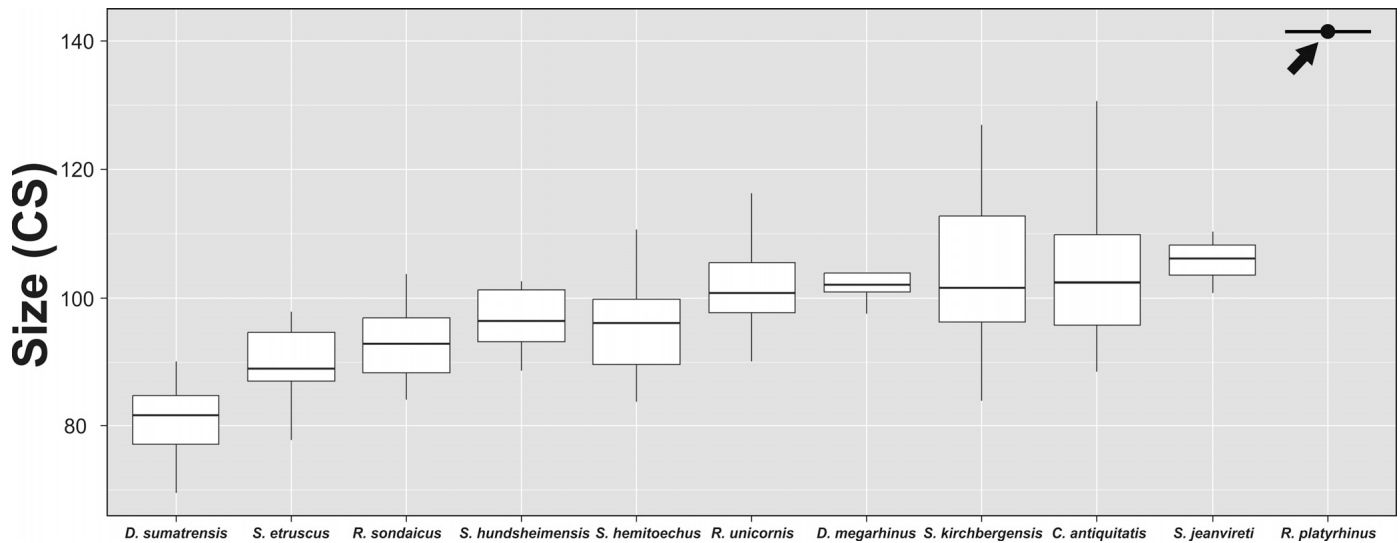


FIGURE 8. Size variation (CS) of skulls of the Plio-Pleistocene Eurasian rhinocerotines. Black arrow indicates *Rhinoceros platyrhinus*.

*Punjabitherium*, which appeared in a trichotomy with *Gaindattherium* and *Rhinoceros* in the phylogenetic relationships proposed by Prothero and colleagues (1986:Fig. 4), and as sister taxon to *Rhinoceros* in the cladogram proposed by Cerdeño (1995: fig. 29). However, the detailed description here provided for NHMUK 36661 and the comparison with several rhinocerotine specimens suggest *Punjabitherium* as a junior synonym of *Rhinoceros*. The diagnostic characters listed by Khan (1971) do not appear sufficient to support a certain attribution to *R. platyrhinus* or to a different genus than *Rhinoceros*. The absence of a nasal septum, the presence of a closed external auditory pseudomeatus, and the presence of two incisors and relatively high-crowned teeth are evident in *R. unicornis*. Contrary to the diagnosis reported by Khan (1971), *R. platyrhinus* does not have a backward-leaning occipital face and the insertion of the frontal horn. Crista and crochet are evident in both *R. platyrhinus* and *R. unicornis*. In addition, when exploring the cranial morphology, *R. platyrhinus* is separated from all other rhinocerotine taxa and lies close to *R. unicornis* at positive PC1 and PC2 values in the cranial morphospace (Fig. 5A). A phenogram of morphological similarities of the skull confirms *R. platyrhinus* as having a similar cranial shape to *R. unicornis* and other extant Asian rhinoceroses (Fig. 7A). Tooth shape analysis reveals that *R. platyrhinus* is much more distinctly a grazer than *R. unicornis* (Fig. 7B). However, *R. platyrhinus* would appear separated from *Rhinoceros* spp. at negative PC3 values (Fig. 6B), even if PC3 explains little variance. Unfortunately, it is impossible to investigate if any shape differences of *R. platyrhinus* occur with other rhinocerotines using a multivariate analysis of variance because there is only one skull of *R. platyrhinus* in the data set.

The results mentioned above support *R. platyrhinus* as being a valid taxon, pertaining to *Rhinoceros*, and most likely sister to *R. unicornis*.

*Rhinoceros unicornis* and *R. platyrhinus* co-occurred during the Pleistocene in the southern Himalayas (Upper Siwaliks). This is not unusual among rhinocerotids; the coexistence of two congeneric species of *Rhinoceros* has been reported in several Middle and Late Pleistocene localities of southeastern Asia (*R. unicornis* and *R. sondaicus*; Antoine, 2012, and references therein). The coexistence of these two latter species may have been possible because of different specializations in diet (Schenkel and Schenkel-Hulliger, 1969; Guérin, 1980; Laurie, 1982; Groves and Leslie, 2011, and references therein). The major differences between *R. unicornis* and *R. sondaicus* are indeed

evident in the teeth, whereas the morphology of the skull is rather similar (Figs. S1–S2; Guérin, 1980). The dental morphology of *R. platyrhinus* resembles that of *R. unicornis*, and the two species differ in the inclination of the occipital face, in the position of the occipital condyles, and in skull size (Fig. S1; Table S2). The orbit is placed posteriorly, and the nasal notch is situated in a more anterior position in *R. platyrhinus* than in *R. unicornis*. These features of Rhinocerotidae that evolved sub-hypsodont or hypsodont teeth (Antoine, 2002), are generally related to siliceous and more abrasive food (e.g., *Coelodonta* and *Ceratotherium*; Guérin, 1980). Morphological changes can be driven by several selective pressures. Upper tooth morphology could have been driven more by ecological adaptation than by shared ancestry, whereas cranial shape change is much more phylogenetically constrained (Piras et al., 2010). Recent findings suggest that teeth are the most evolutionarily labile structures in the crania of Plio-Pleistocene Rhinocerotini in response to dietary regime, as also suggested by the lowest RV values (a metric comparison of covariation between sets of shape variables) found in the morphological integration between the cranial shape in lateral view and upper teeth shape in occlusal view (Piras et al., 2010; Raia et al., 2010).

## CONCLUSIONS

*Rhinoceros platyrhinus* is the largest and one of the rarest rhinocerotine species of the Eurasian Pleistocene. Morphological comparisons and geometric morphometrics show that the skull NHMUK 36661 can be referred to *R. platyrhinus*. New detailed morphological characters are here provided for this species. In addition, comparison with the type material reveals that several specimens previously referred to *R. platyrhinus*, including the lectotype, can be referred to other *Rhinoceros* species such as *R. unicornis* and *R. sivalensis*, or have uncertain specific status (*Rhinoceros* sp.). We suggest that the generic name *Punjabitherium* erected for *R. platyrhinus* represents a junior synonym of *Rhinoceros* due to the morphological affinities of NHMUK 36661 with the type species, *R. unicornis*. The morphological investigation of this specimen adds new data to the evolutionary scenario of the genus *Rhinoceros* in Eurasia. As recently suggested (Singh et al., 2012, 2014), several sub-basins situated south of the Himalayas were characterized by a progressive increase in aridity from ca. 12 Ma to Recent (Singh et al., 2012, 2014). This environmental change could have affected the dietary regime of *R.*

*platyrhinus* towards a more grazer-like diet. Further data are needed to better test this hypothesis.

#### ACKNOWLEDGMENTS

The authors thank P. Agnelli (Museo di Storia Naturale, sezione di Zoologia 'La Specola'), C. Argot and J. Cusin (Muséum National d'Histoire Naturelle), E. Bodor (Geological and Geophysical Institute of Hungary), P. Brewer and R. Portela-Miguez (NHMUK), E. Cioppi (Museo di Storia Naturale, sezione di Geologia-Paleontologia), L. Costeur (Naturhistorisches Museum Basel), F. Farsi (Museo di Storia Naturale Accademia dei Fisiocritici), T. Engel (Naturhistorisches Museum Mainz), M. Fornasiero (Museo di Geologia e Paleontologia di Padova), E. Frey (Staatliches Museum für Naturkunde Karlsruhe), M. Gasparik (Hungarian Natural History Museum), U. Göhlich (Naturhistorisches Museum Wien), R. D. Kahlke (Institut für Quartärpaläontologie), R. Kraft (Zoologische Staatssammlung Munich), K. Kromann (Senckenberg Naturmuseum, Frankfurt), O. Hampe (Museum für Naturkunde, Berlin), R. Manni (Museo di Paleontologia di Roma), P. Monegatti (Museo Paleontologico Parmense), P. Pérez Dios (Museo Nacional de Ciencias Naturales), G. Rössner (Bayerische Staatssammlung für Paläontologie und Geologie, Munich), C. Sarti (Museo di Geologia Giovanni Capellini), and R. Ziegler (Staatliches Museum für Naturkunde Stuttgart) for their help and assistance during the visits to study the rhinoceros fossil collections. L.P. thanks the European Commission's Research Infrastructure Action, EU-SYNTHESYS projects AT-TAF-2550, DE-TAF-3049, GB-TAF-2825, HU-TAF-3593, and ES-TAF-2997. Part of this research received support from the SYNTHESYS Project <http://www.synthesys.info/>, which is financed by European Community Research Infrastructure Action under the FP7 'Capacities' Program. We are also grateful to G. Sansalone for useful suggestions.

#### LITERATURE CITED

- Adams, D. C., F. J. Rohlf, and D. E. Slice. 2004. Geometric morphometrics: ten years of progress following the 'revolution.' *Italian Journal of Zoology* 71:5–16.
- Antoine, P.-O. 2002. Phylogénie et évolution des Elasmotheriina (Mammalia, Rhinocerotidae). *Mémoires du Muséum national d'Histoire naturelle* 188:1–359.
- Antoine, P.-O. 2012. Pleistocene and Holocene rhinocerotids (Mammalia, Perissodactyla) from the Indochinese Peninsula. *Comptes Rendus Palevol* 11:159–168.
- Barry, J. C., A. K. Behrensmeyer, C. E. Badgley, L. J. Flynn, H. Peltonen, I. U. Cheema, D. Pilbeam, E. H. Lindsay, S. M. Raza, A. R. Rajpar, and M. E. Morgan. 2013. The Neogene Siwaliks of the Potwar Plateau, Pakistan; pp. 373–399 in X. Wang, L. J. Flynn, and M. Fortelius (eds.), *Fossil Mammals of Asia: Neogene Biostratigraphy and Chronology*. Columbia University Press, New York.
- Bookstein, F. L. 1986. Size and shape spaces for landmark data in two dimensions. *Statistical Science* 1:181–242.
- Bookstein, F. L. 1991. *Morphometric Tools for Landmark Data: Geometry and Biology*. Cambridge University Press, Cambridge, UK, 456 pp.
- Bookstein, F. L., A. P. Streissguth, P. D. Sampson, P. D. Connor, and H. H. Barr. 2002. Corpus callosum shape and neuropsychological deficits in adult males with heavy fetal alcohol exposure. *NeuroImage* 15:233–251.
- Boulesteix, A. L. 2005. A note on between-group PCA. *International Journal of Pure and Applied Mathematics* 19:359–366.
- Cerdeño, E. 1995. Cladistic analysis of the family Rhinocerotidae (Perissodactyla). *American Museum Novitates* 3143:1–25.
- Colbert, E. H. 1935. Siwalik mammals in the American Museum of Natural History. *Transactions of the American Philosophical Society New Series* 26:1–401.
- Colbert, E. H. 1942. Notes on the lesser one-horned rhinoceros, *Rhinoceros sondaicus*, 2. The position of *Rhinoceros sondaicus* in the phylogeny of the genus *Rhinoceros*. *American Museum Novitates* 1207:1–5.
- Colbert, E. H., and D. A. Hooijer. 1953. Pleistocene mammals from the limestone fissures of Szechwan, China. *Bulletin of the American Museum of Natural History* 102:1–134.
- Desmarest, A. G.. 1822. *Mammalogie, ou description des especes des Mammiferes*. Veuve Agasse, Paris, p. 277–555.
- Falconer, H. 1868. On the species of fossil *Rhinoceros* found in the Sewalik Hills and On the fossil *Rhinoceros* of central Tibet and its relation to the recent upheaval of the Himalayahs; pp. 157–185 in C. Murchison (ed.), *Palaeontological Memoirs and Notes of the late Hugh Falconer* (1) *Fauna Antiqua Sivalensis*. Robert Hardwicke, London.
- Falconer, H., and P. T. Cautley. 1846. *Fauna Antiqua Sivalensis, Being the Fossil Zoology of the Sewalik Hills, in the North of India*. Atlas, Smith, Elder and Co., London, 90 pp.
- Flynn, L. J., E. H. Lindsay, D. Pilbeam, S. M. Raza, M. E. Morgan, J. C. Barry, C. E. Badgley, A. K. Behrensmeyer, I. U. Cheema, A. R. Rajpar, and N. D. Opdyke. 2013. The Siwaliks and Neogene Evolutionary Biology in South Asia; pp. 351–372 in X. Wang, L. J. Flynn, and M. Fortelius (eds.), *Fossil Mammals of Asia: Neogene biostratigraphy and chronology*. Columbia University Press, New York.
- Gray, J. E.. 1821. On the natural arrangement of vertebrate animals. *London Medical Repository* 15:296–310.
- Groves, C. P., and M. Leslie. 2011. *Rhinoceros sondaicus* (Perissodactyla: Rhinocerotidae). *Mammalian Species* 43(887):190–208.
- Guérin, C. 1980. Les rhinocéros (Mammalia, Perissodactyla) du Miocène terminal au Pleistocène supérieur en Europe occidentale: comparaison avec les espèces actuelles. *Documents du Laboratoire de Géologie de la Faculté des Sciences de Lyon* 79:1–1182.
- Khan, A. M., E. Cerdeño, M.A. Khan, and M. Akhtar. 2013. New *Alicornops* (Rhinocerotidae) remains from Lower and Middle Siwaliks, Pakistan. *Annales de Paléontologie* 99:131–155.
- Khan, E. 1971. *Punjabitherium*, gen. nov., an extinct rhinocerotid of the Siwaliks, Punjab, India. *Proceedings of the Indian National Science Academy* 37A:105–109.
- Laurie, A. 1982. Behavioural ecology of the greater one-horned rhinoceros (*Rhinoceros unicornis*). *Journal of Zoology* 196:307–341.
- Linnaeus, C. 1758. *Systema Naturae per regna tria naturae, secundum classes, ordines, genera, species, cum characteribus, differentiis, synonymis, locis*. 10<sup>th</sup> ed. Stockholm, 824 pp.
- Lydekker, R. 1876. Indian Tertiary and post-Tertiary Vertebrata: molar Teeth and other remains of Mammalia. *Memoirs of the Geological Survey of India, Palaeontologica Indica* 10(1):1–69.
- Lydekker, R. 1881. Siwalik Rhinocerotidae. *Palaeontologia Indica* 10(2):1–62.
- Lydekker, R. 1884. *Catalogue of the Remains of Siwalik Vertebrata Contained in the Geological Department of the Indian Museum, Calcutta. Part I, Mammalia*. Superintendent of Government Printing, Calcutta, India, 116 pp.
- Marcus, L. F., E. Hingst-Zaher, and H. Zaher. 2000. Application of landmarks morphometrics to skull representing the orders of living mammals. *Hystrix* 11:27–47.
- Matthew, W. D. 1929. Critical observations upon Siwalik mammals. *Bulletin of the American Museum of Natural History* 56:437–560.
- Matthew, W. D., and W. Granger. 1923. New fossil mammals from the Pliocene of Sze-Chuan, China. *Bulletin of the American Museum of Natural History* 48:563–598.
- Mitteroecker, P., and F. Bookstein. 2011. Linear discrimination, ordination, and the visualization of selection gradients in modern morphometrics. *Evolutionary Biology* 38:100–114.
- Mullin, S. K., and P. J. Taylor. 2002. The effects of parallax on geometric morphometric data. *Computers in Biology and Medicine* 32:455–464.
- Murchison, C. 1867. *Description of the Plates of the Fauna Antiqua Sivalensis from Notes and Memoranda by Hugh Falconer, M.D.* Robert Hardwicke, London, 242 pp.
- Nanda, A. C. 2002. Upper Siwalik mammalian faunas of India and associated events. *Journal of Asian Earth Science* 21:47–58.
- Nanda, A. C. 2008. Comments on the Pinjor Mammalian Fauna of the Siwalik Group in relation to the post-Siwalik faunas of Peninsular India and Indo-Gangetic Plain. *Quaternary International* 192:6–13.
- Owen, R. M. 1848. Description of teeth and proportion of jaws of two extinct Anthracotherioid quadrupeds (*Hyopotamus vectianus* and *Hyopotamus bovinus*) discovered by the Marchioness of Hastings in the Eocene deposits on the N.W. coast of the Isle of Wight: with an

- attempt to develop Cuvier's idea of the classification of pachyderms by the number of their toes. *Quarterly Journal of the Geological Society of London* 4:103–141.
- Owen, R.. 1870. On the fossil remains of mammals found in China. *Quarterly Journal of the Geological Society of London* 26:417–434.
- Perez, S. I., V. Bernal, and P. N. Gonzalez. 2006. Differences between sliding semi-landmark methods in geometric morphometrics, with an application to human craniofacial and dental variation. *Journal of Anatomy* 208:769–784.
- Pilgrim, G. E. 1910. Preliminary note on a revised classification of the Tertiary freshwater deposits of India. *Records of the Geological Survey of India* 40:185–205.
- Pilgrim, G. E. 1913. The correlation of the Siwaliks with mammal horizons of Europe. *Records of the Geological Survey of India* 43:264–326.
- Piras, P., L. Maiorino, P. Raia, F. Marcolini, D. Salvi, L. Vignoli, and T. Kotsakis. 2010. Functional and phylogenetic constraints in Rhinocerotinae craniodental morphology. *Evolutionary Ecology Research* 12:897–928.
- Prothero, D. R., C. Guérin, and E. Manning. 1989. The history of the Rhinocerotidae; pp. 321–340 in D. R. Prothero, E. Manning, and C.-B. Hanson (eds.), *The Evolution of Perissodactyls*, Clarendon Press, New York, and Oxford University Press, London.
- Prothero, D. R., E. Manning, and C.-B. Hanson. 1986. The phylogeny of Rhinocerotidae. *Zoological Journal of the Linnean Society* 87:341–366.
- Raia, P., F. Carotenuto, C. Meloro, P. Piras, and D. Pushkina. 2010. The shape of contention. adaptation, history and contingency in ungulate mandibles. *Evolution* 64:1489–1503.
- Rohlf, F. J. 2013. tpsDig2 version 2.17. Freeware. Available at <http://life.bio.sunysb.edu/morph/>. Accessed December 11, 2013.
- Sansalone, G., T. Kotsakis, and P. Piras. 2016. New systematic insights about Plio-Pleistocene moles from Poland. *Acta Palaeontologica Polonica*. doi: 10.4202/app.00116.2014.
- Schenkel, R., and L. Schenkel-Hulliger. 1969. The Javan rhinoceros (*Rh. sondaicus* Desm.) in Ujung Kulon Nature Reserve. Its ecology and behaviour. *Acta Tropica* 26:97–135.
- Schlager, S. 2013. Morpho: Calculations and Visualizations Related to Geometric Morphometrics. R package version 0.23.3. Available at: <http://CRAN.R-project.org/package=Morpho>. Accessed October 19, 2013.
- Singh, S., B. Parkash, A.K. Awasthi, and T. Singh. 2012. Palaeoprecipitation record using O-isotope studies of the Himalayan Foreland Basin sediments, NW India. *Palaeogeography, Palaeoclimatology, Palaeoecology* 331–332:39–49.
- Singh, S., B. Parkash, A.K. Awasthi, and S. Kumar. 2014. Do stable isotopes in carbonate cement of Mio-Pleistocene Himalayan sediments record palaeoecological and palaeoclimatic changes? *Palaeogeography, Palaeoclimatology, Palaeoecology* 399:363–372.
- Zelditch, M. L., D. L. Swiderski, and H. D. Sheets. 2012. *Geometric Morphometrics for Biologists: A Primer*. Elsevier Academic Press, Amsterdam, The Netherlands, 478 pp.

Submitted February 13, 2015; revisions received June 16, 2015; accepted June 19, 2015.

Handling editor: Anjali Goswami.